

Cite this: *Analyst*, 2012, **137**, 1241

www.rsc.org/analyst

PAPER

## Signal enhancement of a micro-arrayed polydiacetylene (PDA) biosensor using gold nanoparticles

Sang Ho Won<sup>a</sup> and Sang Jun Sim<sup>\*b</sup>

Received 27th September 2011, Accepted 12th December 2011

DOI: 10.1039/c2an15900g

Polydiacetylene (PDA) liposomes possess unique properties that allow liposomes to change color and emit fluorescence in response to stimuli such as temperature, antibody–antigen interaction, pH, mechanical stress, and organic solvent. They have been studied extensively as signal transducers in biosensor applications. Here, we describe an antibody-based biosensor using PDA liposomes for detection of human immunoglobulin E (hIgE). Target hIgE chemically bound to hIgE monoclonal antibodies immobilized on PDA liposomes and the fluorescent signals were slightly increased depending on the target protein concentration. As the primary response, the hIgE could be detected to below 10 ng mL<sup>-1</sup>. However, fluorescent signals were dramatically increased depending on the target protein concentration when gold nanoparticle-conjugated polyclonal antibody probes were added on the PDA liposomes after the primary immune reaction. A PDA liposome biosensor could detect the hIgE as low as 0.1 ng mL<sup>-1</sup> and the sensitivity was increased up to one hundred times higher than the primary response. As a result, we confirmed that gold nanoparticle-conjugated polyclonal antibody probes efficiently enhanced the fluorescent signal of the PDA liposome biosensor chip. This strategy can be useful to detect proteins of ultra-low concentration.

### Introduction

There have been increasing demands for simple, rapid, label-free, and reliable methods for the detection of diseases and using conjugated polymers is a potential solution. Polydiacetylene (PDA) is one of the conjugated polymers that exhibit both blue-to-red colorimetric and nonfluorescent-to-fluorescent transitions when external stimuli, such as temperature, pH, solvents, ions, ligand–receptor interaction, and mechanical perturbations, are applied.<sup>1–6</sup> Because of this unique property, PDAs can be used as biosensors, chemosensors, ion sensors, and temperature sensors.<sup>7–14</sup> In particular, PDA can act as a biosensor for detecting target bio-molecules because of its chromatic and fluorescent properties. Diacetylene monomers have a polar head and an alkyl tail, and they tend to arrange themselves into liposomal structures in aqueous solutions.<sup>15</sup> Closely packed diacetylene monomers can undergo polymerization *via* 1,4-addition reaction upon UV irradiation at 254 nm to form an ene–yne alternating conjugated polymer backbone chain.<sup>16–18</sup> Unperturbed PDA liposomes have long conjugated backbone length and exhibit a blue color. Various external stimuli affect the side chains, which can relieve strain in the ene–yne conjugated

backbone.<sup>19,20</sup> In this state, the PDA absorbs high energy light and exhibits a red color and emits fluorescence. Due to their unique colorimetric response and variation in fluorescent property, PDA-based biosensors can be characterized using UV/visible spectroscopy and fluorescent microscopy.<sup>21</sup>

Allergies were unusual at the turn of the century, but now allergies affect up to 20% of adults and up to 40% of children.<sup>22</sup> Immunoglobulin E (IgE) is the principal triggering mechanism for allergies. In general, the etiology of an allergy is revealed by blood analysis for total and specific IgE levels, which are known to be in direct proportion to the degree of sensitization or severity of disease. The total IgE serum level is widely reported as a marker of atopic diseases, where patient level residues are more than normal clinical values of 290 ng mL<sup>-1</sup> (120 IU mL<sup>-1</sup>).<sup>23,24</sup>

The colorimetric response and signal amplification of PDA liposomes to various external stimuli have been investigated extensively. Our research group has also demonstrated an effective way to enhance the sensitivity and specificity of PDA liposome as a biosensor.<sup>25,26</sup>

In this study, we report the strategy of fluorescent signal enhancement by a polyclonal antibody (pAb) and gold nanoparticles on the PDA liposome biosensor for use in the ultra-sensitive detection of human IgE. This strategy combines the primary antigen–antibody immune reaction and the sandwich method of pAb-conjugated gold nanoparticles.<sup>27</sup> Because PDA liposomes exhibit colorimetric transition and fluorescence due to mechanical stress, we focused on increasing the mechanical

<sup>a</sup>School of Chemical Engineering, Sungkyunkwan University, Suwon, 440-746, Korea

<sup>b</sup>Department of Chemical and Biological Engineering, Korea University, Seoul, 136-713, Korea. E-mail: simsj@korea.ac.kr; Fax: +82-2-926-6102; Tel: +82-2-3290-4853

stress. Our hypothesis is that mechanical stress on PDA liposomes depends on attaching materials weight and pressure. Heavy weight materials will affect the high pressure on PDA liposomes. Therefore, PDA liposomes under high pressure will change their color and fluorescence. Thus, we synthesized different sizes and weights of gold nanoparticles, and then we chose the most effective gold nanoparticles for this experiment. Finally, using gold nanoparticles, conjugated hIgE pAb probes were introduced into the PDA liposome biosensor to enhance the fluorescent signal of PDA liposomes. The response of the PDA liposome spots was then monitored after introduction of target hIgE at various concentrations ( $0.01 \text{ ng mL}^{-1}$  to  $10 \text{ } \mu\text{g mL}^{-1}$ ).

## Experimental

### Materials

10,12-Pentacosadiynoic acid (PCDA), 1,2-dimyristoyl-*sn*-glycero-3-phosphocholine (DMPC), hydrogen tetrachloroaurate ( $\text{HAuCl}_4$ ), sodium citrate ( $\text{Na}_3\text{C}_6\text{H}_5\text{O}_7$ ), 0.1 M phosphate buffer saline pH 7.4 (PBS buffer), bovine serum albumin (BSA), fibrinogen from human plasma, human immunoglobulin G (hIgG), ethylenediamine, *N*-hydroxysuccinimide (NHS), *N*-ethyl-*N*-(3-diethylaminopropyl) carbodiimide hydrochloride (EDC), HPLC-grade chloroform, and ethanol were purchased from Sigma-Aldrich (Korea).  $\text{HS}(\text{CH}_2)_{11}(\text{OCH}_2\text{CH}_2)_6\text{OCH}_2\text{COOH}$  (HS-OEG<sub>6</sub>-COOH) and  $\text{HS}(\text{CH}_2)_{11}(\text{OCH}_2\text{CH}_2)_3\text{OH}$  (HS-OEG<sub>3</sub>-OH) were purchased from Cos Biotech (Daejeon, Korea). Monoclonal human IgE antigen, monoclonal human IgE antibody (hIgE mAb), and polyclonal human IgE antibody (hIgE pAb) were supplied by Fitzgerald Industries International Inc. (MA, USA). Amine-coated glass was supplied by GS-Nanotech (Masan, Korea). Deionized water (DI, resistance of water was  $18.2 \text{ m}\Omega \text{ cm}^{-1}$ ), obtained from a water purification system (Human Corporation, Korea), was used for preparation of washing and buffer solutions.

### Experimental methods

**Immobilization of PDA liposomes on the amine-coated glass surface.** Chloroform solutions of PCDA and DMPC were prepared separately in amber glass vials at  $-4 \text{ }^\circ\text{C}$ . Solutions of the two lipid monomers were mixed in 8 : 2 molar ratios (PCDA : DMPC) to a total lipid concentration of 1.0 mM. After the chloroform was removed with  $\text{N}_2$  gas, the remaining dry film of mixed diacetylene was resuspended in 1.0 mL of 10 mM PBS buffer (pH 7.4) by heating in a circulating water bath set at  $80 \text{ }^\circ\text{C}$  for 15 min with gentle stirring. The prepared solution was repeatedly extruded through a prefilter–100 nm membrane–prefilter complex. The extruder system was kept at  $85 \text{ }^\circ\text{C}$  for the PCDA and DMPC lipid formation on the dry bath. The extruded solution had 100 nm liposomes. The liposome solution was then cooled for 20 min to room temperature ( $25 \text{ }^\circ\text{C}$ ). The NHS and EDC were dissolved separately in PBS buffer to a total concentration of 200 mM. Ethylenediamine (total concentration of 1.0 mM) and NHS/EDC (equal volume ratios) solutions were then added to the liposome solution. The solutions were arrayed by an automated liquid handling system (Aurora Biomed) at room temperature at 4 spots per well, with 8 wells per amine-coated glass. The spot out of 8 wells was designated as ‘control

areas’ in which only PBS buffer on hIgE mAb-modified PDA spots was added. The PDA liposome-arrayed glass was then incubated in a chamber for 2 h at a constant temperature of  $4 \text{ }^\circ\text{C}$ . Interlinking and immobilization of the liposomes occurred during incubation, after which the PDA liposome-arrayed glass was repeatedly washed with deionized water and 0.1% Tween-20 in water, followed by soft drying under a stream of pure  $\text{N}_2$  gas.

### Preparation of gold nanoparticles and gold nanoparticle–hIgE pAb probes.

Gold nanoparticles were synthesized by sodium citrate reduction of aqueous  $\text{HAuCl}_4$  solution.<sup>28</sup> A volume of 20 mL of 1.0 mM  $\text{HAuCl}_4$  was heated to boiling, and 2 mL, 1.5 mL, and 1 mL of 1% sodium citrate were added to the boiling solution, while stirring vigorously. Then each solution was further boiled for 5 min to complete the citrate reduction of gold ions. Each solution was cooled to room temperature for 30 min with stirring. This method yields spherical ruby red particles with an average diameter of approximately 13 nm, 25 nm, or 52 nm (Fig. 2). The size and morphology of the synthesized gold nanoparticles were estimated by high-resolution transmission electron microscopy (HR-TEM, JEOL JEM-3011 operated at 300 kV). After synthesis of the colloidal solution, HS-OEG<sub>6</sub>-COOH/HS-OEG<sub>3</sub>-OH capped gold nanoparticle solution was obtained through displacement of citrate by a relatively short and negatively charged thiol that exhibits strong interactions with gold.<sup>29</sup> The gold nanoparticles were capped with a 1 : 10 molar ratio of HS-OEG<sub>6</sub>-COOH/HS-OEG<sub>3</sub>-OH by mixing 9 mL gold solution and 1 mL ethanolic solution of HS-OEG<sub>6</sub>-COOH/HS-OEG<sub>3</sub>-OH to yield an effective HS-OEG<sub>6</sub>-COOH/HS-OEG<sub>3</sub>-OH capping concentration of 0.5 mM. After gentle stirring for 6 h at room temperature, the mixed solution was washed to separate unbound HS-OEG<sub>6</sub>-COOH/HS-OEG<sub>3</sub>-OH from the carboxylated gold nanoparticles by centrifugation for 15 min at 14 000 rpm. The pellet was then resuspended in 0.1 M PBS buffer (pH 7.4). The washing step was repeated three times. The carboxylated gold nanoparticles were stored in 0.1 M PBS buffer at  $4 \text{ }^\circ\text{C}$ . To prepare gold nanoparticle–hIgE pAb probes, 1 mL of carboxylated gold nanoparticles was mixed with 10  $\mu\text{L}$  of 0.1 M EDC/NHS. Immediately, 100  $\mu\text{L}$  of hIgE pAb ( $10 \text{ } \mu\text{g mL}^{-1}$ , dialyzed in PBS pH 7.4) was added to the activated gold nanoparticles. The solution was mixed well, and then it was allowed to react for at least 2 h at ambient temperature with gentle mixing. Finally, gold nanoparticle–hIgE pAb probes were rinsed, collected, and stored in 0.1 M PBS buffer (pH 7.4) at  $4 \text{ }^\circ\text{C}$  for further experiments.

### Conjugation of gold nanoparticles onto a PDA liposome chip.

After PDA liposome immobilization, the PDA liposome spot was polymerized under 254 nm UV light at  $1.0 \text{ mW cm}^{-2}$  intensity for 10 min. The NHS/EDC was dissolved in the PBS buffer (200 mM) and the three kinds of carboxylated gold nanoparticles were added separately to the solution. Detection spots were conjugated with gold nanoparticles by an automated liquid handling system. After spotting the gold nanoparticles, the PDA liposome-arrayed glass was incubated in a chamber at  $4 \text{ }^\circ\text{C}$  for 3 h, then washed gently with deionized water and dried with pure  $\text{N}_2$  gas. After the washing step, each fluorescent signal was analyzed by fluorescent microscopy. The fluorescent microscope consisted of four major parts: a microscope, a fluorescent unit

(composed of a mercury arc lamp as a light source, a fluorescent attachment, and a Nikon G2A filter suitable for analysis of red phase PDA fluorescence), a digital camera unit (Infinity, USA), and image analysis software (*i-solution*, Korea). Fluorescent signals from the PDA liposome spots were visualized with this system and digital micrographs were taken. Spot intensities were calculated with the image analysis software. Intensity denotes the average intensity value of each pixel and was between 0 and 255, as analyzed by the digital image analysis, where 0 was the minimum and 255 was the maximum. All fluorescent signal data in this paper are presented as the resulting value from the output signal subtracted from the baseline signal derived from the reaction with buffer.

**Conjugation of hIgE mAb onto a PDA liposome chip.** The immobilized PDA liposome on amine-coated glass was polymerized under 254 nm UV light at  $1.0 \text{ mW cm}^{-2}$  intensity for 10 min. The NHS/EDC was dissolved in the PBS buffer (200 mM) and the hIgE mAb added to the solution. Detection spots were conjugated with the antibody by an automated liquid handling system. After spotting the antibody, the PDA liposome-arrayed glass was incubated in a chamber at  $4 \text{ }^\circ\text{C}$  for 3 h, then washed gently with deionized water and dried with pure  $\text{N}_2$  gas.

**Performance of immunoreactions and fluorescent analysis for the hIgE detection.** After 5.0 nM of hIgE mAb was added to the PDA liposome spots, the hIgE was diluted to various concentrations. Each protein was then dropped on the PDA liposome spots and the chip was incubated at  $37 \text{ }^\circ\text{C}$  for 30 min. The PBS buffer was added to the PDA liposome conjugated as a baseline. After 30 min, the fluorescent signal was analyzed by fluorescent microscopy.

**Detection of the hIgE by signal enhancement using gold nanoparticle–hIgE pAb probes.** Enhancement of the PDA liposome signal was investigated using a sandwich immunoassay. After the immune response between the hIgE and mAb occurred, gold nanoparticle–hIgE pAb probes ( $100 \text{ } \mu\text{g mL}^{-1}$  in PBS buffer) were dropped on the PDA liposome, conjugated, and incubated for 30 min at  $37 \text{ }^\circ\text{C}$  for the enhancement step. After incubation, fluorescent change was analyzed by fluorescent microscopy.

**Specificity and selectivity test of target hIgE on a PDA liposome biosensor.** Using a PDA liposome biosensor treated with hIgE antibody, the specificity and selectivity of the target proteins were tested on prepared PDA liposome biosensors. First, the BSA, fibrinogen, hIgG, and hIgE were diluted to  $1.0 \text{ } \mu\text{g mL}^{-1}$  concentrations. Then, each protein was dropped onto the wells of the PDA liposome biosensors and incubated at  $37 \text{ }^\circ\text{C}$  for 30 min. The PBS buffer was then added onto the antibody-modified PDA liposome spots as a baseline.

## Result and discussion

This experiment consists of two stages. The first stage is choosing the most effective gold nanoparticles for signal amplification as shown in Fig. 1(A). The second stage is detection of the hIgE target molecules at ultra-low concentration using hIgE pAb-conjugated gold nanoparticles which were chosen at the first stage as shown in Fig. 1(B). Three different sizes of gold nanoparticles were fabricated in this investigation to determine which size had the most effective stimulus on PDA liposomes. The gold nanoparticles with different diameters were prepared by controlling the amount of sodium citrate reducing agent. Fig. 2 shows absorption spectra of three different sizes of gold

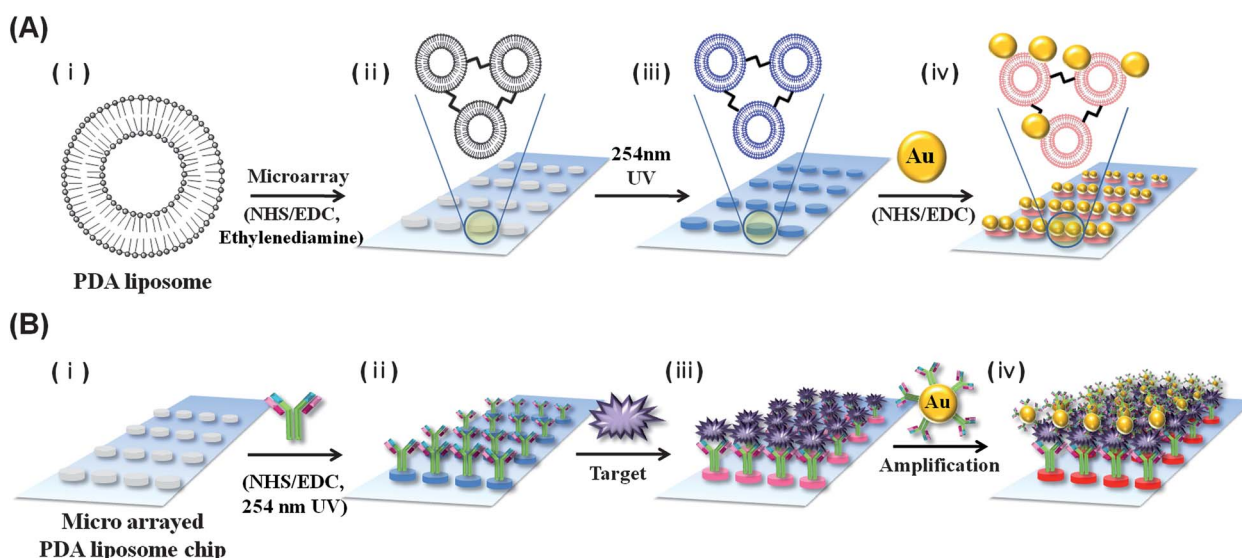


**Fig. 1** (A) Schematic diagram illustrating the fabrication steps for gold nanoparticle conjugation on PDA liposomes. (i) Preparation of the PDA liposome included PCDA and DMPC. (ii) Immobilization of PDA liposome onto the amine-coated glass through NHS-activated carboxylic acid–amine coupling. Ethylenediamine was then added to cross-link the PDA liposomes. (iii) PDA liposomes were polymerized under 254 nm UV light. (iv) Conjugation of gold nanoparticles onto the liposome chip. (B) Schematic diagram illustrating the fabrication steps in the biosensor based on PDA liposomes for detection of hIgE. (i) Immobilization of PDA liposomes onto amine-coated glass. (ii) After treatment of the liposome surface with NHS/EDC, the monoclonal hIgE antibodies were immobilized onto the PDA liposome surface. (iii) The analytes (hIgE) were then combined on the PDA liposome surface. (iv) Finally, gold nanoparticle conjugated polyclonal hIgE antibody probes for signal amplification were added onto the PDA liposome surface.



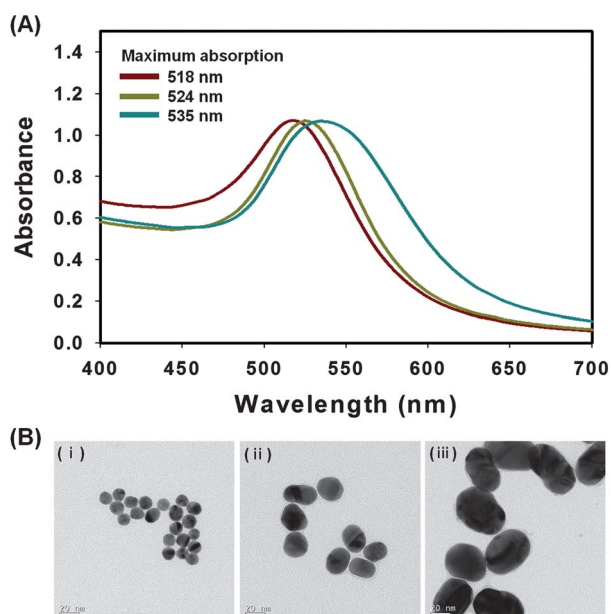


**Fig. 2** (A) UV-vis absorption spectra of each gold nanoparticle. (B) HR-TEM images of each gold nanoparticle. The average diameter of gold nanoparticles is (i) 13 nm, (ii) 25 nm, and (iii) 52 nm, respectively.

nanoparticles and high-resolution transmission electron microscopy (HR-TEM) images of each. We estimated the size and morphology of gold nanoparticles by using a UV spectrometer and HR-TEM. The absorption spectra of these gold nanoparticles were measured by using a UV spectrometer. The absorption peaks were red shifted with increased diameter. The sizes of gold nanoparticles were determined as mean values by counting three to five representative regions within each image by HR-TEM. As a result, average diameters of  $12.6 \pm 0.7$  nm,  $24.5 \pm 1.7$  nm, and  $52.4 \pm 5.1$  nm were obtained.

A mixture consisting of PCDA as the major component and DMPC yielded a liposome with the carboxylate functional group of PCDA. This liposome was immediately modified with NHS and EDC, replacing the carboxyl group with an amine-reactive NHS-ester moiety. The activated PDA liposomes were arrayed onto an amine-coated glass surface and polymerized under UV light (254 nm) for 10 min. Each carboxyl functionalized gold nanoparticle solution containing the same concentration (optical density = 1.071) was prepared because we focused on the mechanical stress due to gold nanoparticle size and weight.

To induce fluorescence by mechanical stimulus, the carboxylated gold nanoparticle solution was added and the chip incubated at  $4^\circ\text{C}$  for 3 h. Fig. 3 shows the fluorescent responses of the chip and the fluorescent spot images depending on gold nanoparticle size. The fluorescent signal was highest with the 52 nm size of gold nanoparticles. The larger gold nanoparticles are heavier and exert more pressure on PDA liposomes. Therefore, using large gold nanoparticles is most effective in the mechanical stimulation of PDA liposomes.

The PDA liposomes were conjugated with the hIgE mAb and their fluorescent signals were monitored at target hIgE concentrations between  $0.01\text{ ng mL}^{-1}$  and  $10\,000\text{ ng mL}^{-1}$  in PBS buffer (pH 7.4). Before detection of hIgE, we optimized the hIgE mAb concentration. The fluorescent signal indicated the highest and

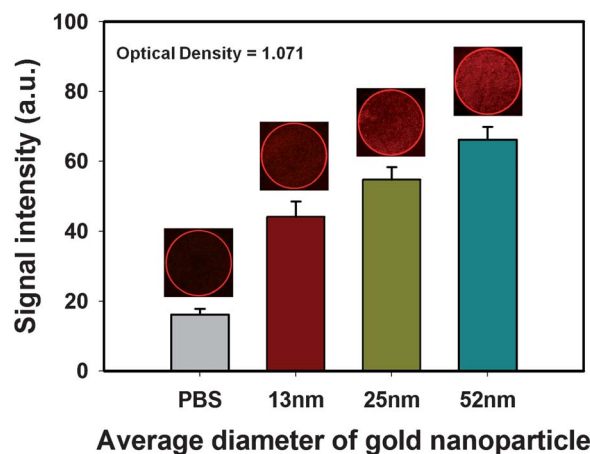


**Fig. 3** Fluorescent microscopy images and fluorescent signals of immobilized PDA spots when the three different sizes of gold nanoparticles were conjugated on PDA liposomes.

most efficient responses at the hIgE mAb concentration of  $5.0\text{ ng mL}^{-1}$  (data not shown). The blue-colored bars in Fig. 4 show the fluorescent intensity and images of PDA liposome spots after interaction between the target hIgE and hIgE mAb. In this case, the fluorescent signals increased stepwise upon contact with hIgE at concentrations increasing from 10 to  $10\,000\text{ ng mL}^{-1}$ . However, the analytes of concentrations below  $10\text{ ng mL}^{-1}$  were not determined. The calibration curves for hIgE detection obtained using the antibody-modified PDA liposome chips are

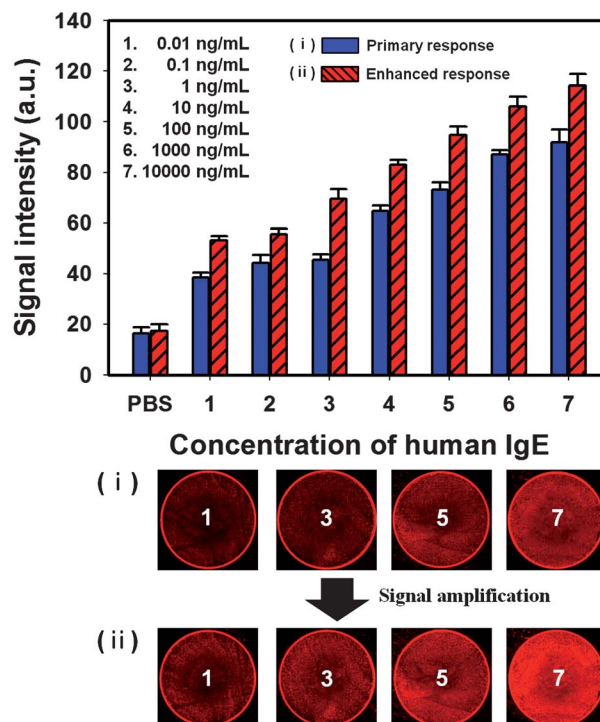


**Fig. 4** Fluorescent microscopy images of immobilized PDA spots when the target hIgE, after hIgE mAb immobilization, was conjugated on the PDA liposomes and a diagram representing the fluorescent signals with (i) primary response (blue bars) and (ii) enhanced response (red bars) after 30 min incubation at  $37^\circ\text{C}$ .

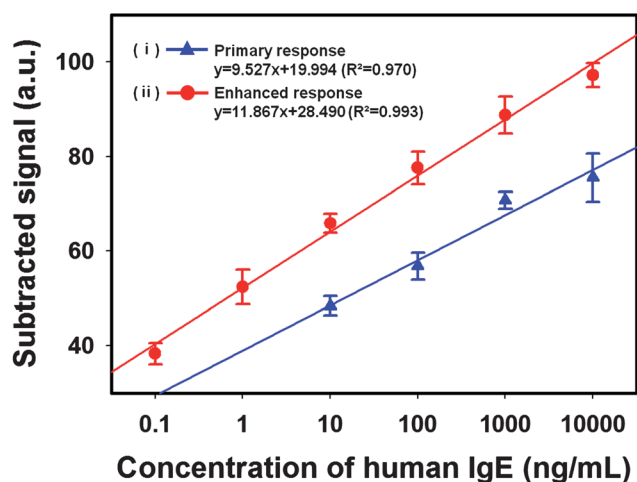


**Fig. 5** Linear plot of the fluorescence response of hIgE in mixture solution. The two lines indicate: (i) primary response and (ii) enhanced response of the PDA liposomes. (Error bars illustrate relative standard deviation (RSD). The subtracted signal is the resulting value from the output signal subtracted from the baseline signal derived from the reaction with PBS buffer,  $n = 5$ .)

shown in Fig. 5. The linear regression equation for hIgE detection by the interaction of hIgE and hIgE mAb was:  $y = 9.527x + 19.994$  ( $R^2 = 0.970$ ), where  $y$  and  $x$  are the fluorescent signals of the PDA liposome and analysis (hIgE) concentration ( $\text{ng mL}^{-1}$ ), respectively.

In the case of the primary response alone, the linear dynamic range was from 10 to 10 000  $\text{ng mL}^{-1}$  and the detectable minimum concentration was 10  $\text{ng mL}^{-1}$ . The hIgE antibody modified PDA liposome system by the primary response is possible for real detection of hIgE because allergic patients have a total serum hIgE higher than 290  $\text{ng mL}^{-1}$ . However, this

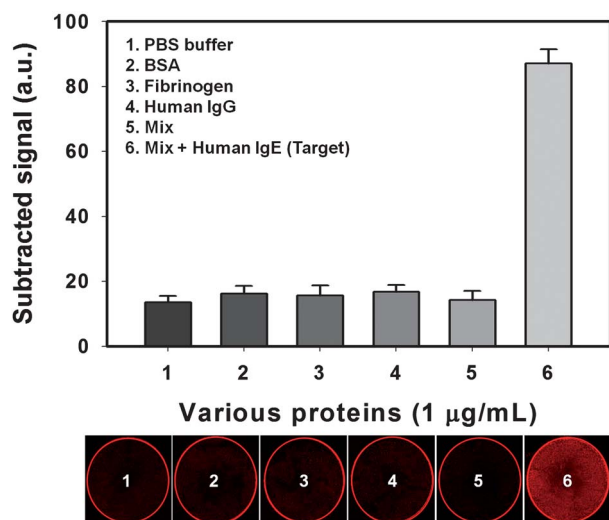


**Fig. 6** Specificity and selectivity of the hIgE mAb for target hIgE detection. The adsorptions of bovine serum albumin (BSA), fibrinogen, and human immunoglobulin G (hIgG) were added independently and were negligible, as with PBS buffer. (The subtracted signal is the resulting value from the output signal subtracted from the baseline signal derived from the reaction with PBS buffer,  $n = 5$ .)

antibody based PDA liposome system could detect hIgE at ultra-low concentrations by the secondary response. To increase the sensitivity of PDA chips, other selective stimuli such as mechanical force should be introduced onto PDA liposomes.

To achieve ultra-sensitive detection of target hIgE with an antibody-modified PDA biosensor, polyclonal hIgE antibody (hIgE pAb) conjugated 52 nm sized gold nanoparticles were used as external stimuli for the secondary response. After the immune reaction between target hIgE and antibody-modified PDA liposomes occurred, gold nanoparticle-hIgE pAb probes ( $10 \mu\text{g mL}^{-1}$  in PBS buffer) were dropped on the PDA liposomes at  $37^\circ\text{C}$  for fluorescent signal enhancement. The red-colored bars in Fig. 5 show the fluorescent intensity of PDA liposome spots after the addition of mechanical force with gold nanoparticle-hIgE pAb probes. In the case of enhanced signal, the fluorescent signals also increased stepwise upon contact with hIgE at various concentrations increasing from 0.1 to 10 000  $\text{ng mL}^{-1}$ . However, the analytes were not determined at concentrations below 0.01  $\text{ng mL}^{-1}$ . A linear regression equation for the enhanced response was calculated as:  $y = 11.867x + 28.490$  ( $R^2 = 0.993$ ), as shown in Fig. 5. In the case of enhanced response, the linear dynamic range was from 0.1 to 10 000  $\text{ng mL}^{-1}$  and the detectable minimum concentration was 0.1  $\text{ng mL}^{-1}$ . These results show that the sensitivity and dynamic range of PDA liposome chips could be effectively improved by the mechanical force using gold nanoparticle-hIgE pAb probes.

An antibody-modified PDA liposome biosensor was analyzed in a mixed solution containing BSA, fibrinogen, and hIgG to investigate nonspecific adsorption and selectivity of target proteins. These nontarget proteins ( $1.0 \mu\text{g mL}^{-1}$ ) and PBS buffer (pH 7.4) were injected onto the hIgE mAb-conjugated PDA liposome spots to examine for nonspecific binding of the chip. In addition, an experiment was conducted to investigate the selectivity of the biosensor using mixed solutions of various nontarget proteins ( $1.0 \mu\text{g mL}^{-1}$ ), PBS buffer (pH 7.4), and target IgE ( $1.0 \mu\text{g mL}^{-1}$ ). As shown in Fig. 6, after the nontarget proteins were injected onto the PDA liposome chip, the fluorescent intensities of all proteins increased slightly, as with PBS buffer. As a result, nonspecific adsorption of the nontarget proteins was negligible, even at very high concentrations. On the other hand, the fluorescent intensity was significantly increased in the mixture solution with hIgE target protein. Therefore, the target protein can be detected selectively at low concentrations in the presence of high concentrations of nontarget proteins by the antibody-modified PDA liposome biosensors.

## Conclusions

In this study, a novel PDA-based fluorescent micro-array chip procedure has been developed for label free detection of allergy diagnosis. External stimuli induce the ene-yne backbone perturbation of the PDA liposome. This event triggers the color change from blue to red and also produces red fluorescence emission of the PDA liposome. To demonstrate the signal enhancement mechanism by a mechanical force effect on the PDA liposome, three different sizes of gold nanoparticles were synthesized and conjugated onto the PDA liposome at the same concentration. We confirmed that the fluorescent signal was highest with the largest gold nanoparticles because they could

easily stimulate the PDA liposome by their heavy weight and high pressure. Afterward gold nanoparticle-conjugated polyclonal antibody probes were used to accomplish ultra-sensitive protein detection on the PDA liposome biosensor. The signal amplification response is due to the increasing external mechanical perturbations due to the weight and pressure of gold nanoparticles. As a result, sensitivity as low as  $0.1 \text{ ng mL}^{-1}$  for detection of hIgE was obtained for the PDA liposome biosensor and the detection limit was one hundred times lower than that of the detection method without signal amplification. We successfully demonstrated the fluorescent signal enhancement of PDA biochips using this sandwich method. Finally, we have developed a highly selective and sensitive quantitative PDA liposome-based sensor system. This strategy can be applied to the diagnosis of events associated with many kinds of proteins at ultra-low concentrations.

## Acknowledgements

This work was supported by the National Research Foundation of Korea (NRF) grant funded by the Korea government (MEST) (grant no. R0A-2008-000-20078-0/2010-0027771/2010-0027955) and the grant from the Advanced Biomass R&D Center (ABC) of Korea (grant no. 2010-0029728), funded by the Ministry of Science and Technology of the Korean government of the Republic of Korea.

## Notes and references

- 1 R. R. Chance, R. H. Baughman, H. Muller and C. J. Eckhardt, *J. Chem. Phys.*, 1977, **67**, 3616–3618.
- 2 R. R. Chance, *Macromolecules*, 1980, **13**, 396–398.
- 3 R. A. Nallicheri and M. F. Rubner, *Macromolecules*, 1991, **24**, 517–525.
- 4 N. Mino, H. Tamuara and K. Okawa, *Langmuir*, 1992, **8**, 594–598.
- 5 S. Okada, S. Peng, W. Spevak and D. Charych, *Acc. Chem. Res.*, 1998, **31**, 229–239.
- 6 D. J. Ahn, E. Chae, G. S. Lee and H. Shim, *J. Am. Chem. Soc.*, 2003, **125**, 8976–8977.
- 7 I. Gill and A. Ballesteros, *Angew. Chem., Int. Ed.*, 2003, **115**, 3386–3389.
- 8 X. Chen, S. Kang, M. J. Kim, J. Kim, Y. S. Kim, H. Kim, B. Chi, S. J. Kim, J. Y. Lee and J. Yoon, *Angew. Chem., Int. Ed.*, 2010, **49**, 1422–1425.
- 9 M. A. Reppy and B. A. Pindzola, *Chem. Commun.*, 2007, 4317–4338.
- 10 Y. Scindia, L. Silbert, R. Volinsky, S. Kolusheva and R. Jelinek, *Langmuir*, 2007, **23**, 4682–4687.
- 11 J. Lee, H. J. Kim and J. Kim, *J. Am. Chem. Soc.*, 2008, **130**, 5010–5011.
- 12 S. Kolusheva, R. Kafri, M. Katz and R. Jelinek, *J. Am. Chem. Soc.*, 2001, **123**, 417–422.
- 13 D. J. Ahn, S. Lee and J. M. Kim, *Adv. Funct. Mater.*, 2009, **19**, 1483–1496.
- 14 M. L. Guo, G. Guo, J. Zhang, K. Men, J. Song, F. Luo, X. Zhao, Z. Y. Qian and Y. Q. Wei, *Sens. Actuators, B*, 2010, **150**, 406–411.
- 15 N. Charoenthai, T. Pattanatornchai, S. Wacharasindhu, M. Sukwattanasitt and R. Traiphol, *J. Colloid Interface Sci.*, 2011, **360**, 565–573.
- 16 B. Chu and R. Xu, *Acc. Chem. Res.*, 1991, **24**, 384–389.
- 17 Q. Huo, K. C. Russell and R. M. Leblanc, *Langmuir*, 1999, **15**, 3972–3980.
- 18 J. M. Kim, E. K. Ji, S. M. Woo, H. W. Lee and D. J. Ahn, *Adv. Mater.*, 2003, **15**, 1118–1121.
- 19 X. Guo, J. E. Whitten and D. J. Sandman, *J. Chem. Phys.*, 2007, **126**, 184905.
- 20 D. Lee, S. K. Sahoo, A. L. Cholli and D. J. Sandman, *Macromolecules*, 2002, **35**, 4347–4355.
- 21 H. G. Park, A. Gokarna, J. P. Hulme and B. H. Chung, *Nanotechnology*, 2008, **19**, 235103.
- 22 W. E. Winter, N. S. Hardt and S. Fuhrman, *Arch. Pathol. Lab. Med.*, 2000, **124**, 1382–1385.
- 23 D. R. Jackola, M. N. Blumenthal and A. Rosenberg, *Hum. Immunol.*, 2004, **65**, 20–30.
- 24 L. B. Buravkova, M. P. Rykova, Y. G. Gertsik and E. N. Antropova, *Acta Astronaut.*, 2007, **60**, 254–258.
- 25 I. K. Kwon, J. P. Kim and S. J. Sim, *Biosens. Bioelectron.*, 2010, **26**, 1548–1553.
- 26 J. P. Kim, I. K. Kwon and S. J. Sim, *Biosens. Bioelectron.*, 2011, **26**, 4823–4827.
- 27 J. S. Park, M. K. Cho, E. J. Lee, K. Y. Ahn, K. E. Lee, J. H. Jung, Y. J. Cho, S. S. Han, Y. K. Kim and J. Lee, *Nat. Nanotechnol.*, 2009, **4**, 259–264.
- 28 J. Turkevich, P. C. Stevenson and J. Hiller, *Discuss. Faraday Soc.*, 1951, **11**, 55–59.
- 29 S. Y. Lin, Y. T. Tsai, C. C. Chen, C. M. Lin and C. H. Chen, *J. Phys. Chem. B*, 2004, **108**, 2134–2139.